

Unsupervised Anomaly Detection for Aircraft PRSOV With Random Projection-Based Inner Product Prediction

Dandan Peng^{ID}, Ning Zhu^{ID}, Te Han^{ID}, Member, IEEE, Zhuyun Chen^{ID}, Member, IEEE, and Chenyu Liu^{ID}

Abstract—Pressure-regulated shutoff valves (PRSOVs) are critical components of aircrafts' environmental control system (ECS) to regulate the carbon pressure, ensuring it within a safe and comfortable range. However, due to the harsh and dynamic operational environment, PRSOVs are susceptible to various anomalies, which may lead to severe flight incidents such as cabin depressurization. To this end, this article proposed an unsupervised anomaly detection approach for PRSOV with random projection-based inner product prediction (RPDP-AD). It leverages distance information in a randomly projected space to construct supervisory signals. This enables our model to encode distribution patterns and data structures of normal samples from unlabeled data. Our model is optimized to minimize the prediction errors in the random projection space. We introduced a distribution difference metric to minimize the discrepancy between learnable mappings and random mappings in low-dimensional space. Anomalous samples will have greater distribution differences, which allow for unsupervised anomaly detection (UAD). This article explored the connection between neural networks and random projection theory for industrial anomaly detection. To further support its effectiveness, we also provide a theoretical analysis of inner product preservation property via Johnson-Lindenstrauss theorem. Experiments were conducted on a PRSOV dataset including seven types of anomalies with different random projection methods. Results demonstrate that our method outperforms other data-driven counterparts. Our source code will be available at <https://github.com/Z-yiwei/RPDP-AD>

Index Terms—Anomaly detection, deep learning, fault diagnosis, pressure regulated shutoff valves (PRSOVs).

I. INTRODUCTION

AIR transport is the most convenient mode of modern transportation, which significantly boosts global

Received 18 December 2024; revised 2 March 2025; accepted 21 March 2025. Date of publication 16 May 2025; date of current version 30 May 2025. This work was supported in part by the Fundamental Research Funds for the Central Universities, Northwestern Polytechnical University under Grant G2023KY05102; in part by the National Natural Science Foundation of China under Grant 72201152 and Grant 52205101; and in part by the Innovation Fund of Glasgow College, University of Electronic Science and Technology of China. The Associate Editor coordinating the review process was Dr. Siliang Lu. (*Dandan Peng and Ning Zhu contributed equally to this work.*) (*Corresponding author: Chenyu Liu.*)

Dandan Peng is with the Department of Electrical and Electronic Engineering, The Hong Kong Polytechnic University, Hong Kong, China.

Ning Zhu is with the Glasgow College, University of Electronic Science and Technology of China, Chengdu 611731, China.

Te Han is with the Center for Energy and Environmental Policy Research, Beijing Institute of Technology, Beijing 100081, China.

Zhuyun Chen is with the School of Electromechanical Engineering, Guangdong University of Technology, Guangzhou 510520, China.

Chenyu Liu is with the School of Mechanical Engineering, Northwestern Polytechnical University, Xi'an 710072, China (e-mail: chenyuliu@nwpu.edu.cn).

Digital Object Identifier 10.1109/TIM.2025.3568969

economic activities and interpersonal connections. During flight, aircraft may experience drastic changes in operating conditions such as speed, temperature, humidity, and air pressure. These variations could lead to degradation, abnormalities in some core components, posing significant challenges to aircraft operation and maintenance [1], [2]. The pressure-regulated shutoff valves (PRSOVs) are key components of aircrafts' environmental control system (ECS). They regulate and control gas and help to ensure that appropriate amounts of hot air are introduced into the ECS under varying flight phases and environmental conditions [3]. If a PRSOV fails, it may lead to cabin depressurization and temperature loss, which could result in aviation safety incidents. To address these risks, a reliable and precise prognostics and health management system is highly important [4], [5]. Such systems monitor the health conditions of core aircraft components to reduce unscheduled maintenance, enhance flight safety, and lower operational risks [6].

Aircraft are equipped with hundreds or even thousands of sensors to monitor various states during operation. To process this vast amount of data, data-driven algorithms are widely used for the health monitoring and diagnostics of critical aircraft components [7], [8]. In the early stages, researchers primarily relied on experience to identify and assess abnormal aircraft states. This was achieved by setting thresholds or using specific logical rules [9], [10]. However, their efficacy was limited when handling complex systems and large-scale data.

To handle cases with increasing complexity and difficulty, feature engineering has become a critical step in related algorithm development. Researchers have proposed various feature extraction algorithms to capture representative fault features from high-dimensional data by utilizing domain knowledge and data characteristics. Techniques such as Fourier transform and wavelet transform have been employed to extract features from signals [11], [12], [13]. These features are then fed into machine-learning-based decision models to achieve intelligent diagnostics [14], [15], [16]. However, the aforementioned methods also have limitations. Manual feature engineering heavily relies on expert experience, introducing bias and failing to fully capture the dynamic nature of aircraft systems. On the other hand, traditional machine learning algorithms, with their limited nonlinear capabilities, struggle to handle high-dimensional and large-scale datasets.

In recent years, deep learning has provided another effective alternative with a stronger ability to learn complex features, which have become a widely adopted auxiliary tool for aircraft fault detection and diagnosis. PRSOV, as a crucial

component of the aircraft, has attracted researchers' attention [23]. However, this success heavily depends on large amounts of labeled anomalous data. In real-world operations, due to the rarity and diversity of faults, it is nearly impossible to obtain large, labeled datasets covering all fault categories. Moreover, precise labeling that covers all required fault types is both time-consuming and expensive; therefore, unsupervised anomaly detection (UAD) has received considerable attention. This approach aims to automatically extract representative features only from normal data by designing self-supervised proxy tasks. It learns the distribution characteristics and inner latent structures of normal data in a label-free manner, and its training process does not rely on any anomalous data. However, our analysis reveals three critical gaps in PRSOV-specific applications. First, within the scope of our research, although great success has been achieved in UAD for industrial applications [17], [18], [19], [20], [21], [22], UAD specifically designed in a label-free manner for PRSOV has been scarcely discussed. Second, directly deploying existing UAD methods to PRSOV also poses great challenges. State-of-the-art architectures like transformer-based models require more computational resources than typical avionics processors can provide. Third, most methods lack theoretical guarantees, which are a significant limitation given the strict reliability requirements in aerospace systems.

To resolve these issues, random projection theory provides meaningful insight. Random projection is a dimensionality reduction technique that uses a random projection matrix to project high-dimensional data into a lower-dimensional space while approximately preserving the distances between data points [17]. In high-dimensional spaces, the relative positions and distances between data points reflect their similarities and differences. By maintaining these distance relationships, the algorithm retains the structure and characteristics of the original data. Random projection has been explored to be combined with deep learning techniques in various tasks. However, its potential for unsupervised industrial anomaly detection has been theoretically analyzed.

To address the challenges of UAD and further explore the potential of deep learning-based random projection theory in industrial anomaly detection, this article introduces RPDP-AD: an unsupervised PRSOV multifault Anomaly Detection algorithm based on Random Projection Distance Prediction. Anomaly detection approach for PRSOV with random projection-based inner product prediction (RPDP-AD) utilizes distance information in the randomly projected space to construct supervisory signals, allowing the model to encode the data structure and distribution patterns of normal samples from unlabeled data in an unsupervised manner. A distribution difference metric is also introduced to minimize the discrepancy between learnable mappings and random mappings in the low-dimensional space. Unlike existing deep learning methods that learn deterministic embeddings, our framework preserves theoretical interpretability through fixed random mappings while enabling adaptive feature learning via trainable projection heads. To our best knowledge, this represents the first systematic attempt to combine random projection theory with deep neural networks for industrial anomaly detection,

especially in aviation component monitoring. To provide a theoretical foundation, we also conduct a theoretical analysis of the inner product preservation property based on the Johnson–Lindenstrauss theorem to demonstrate the feasibility of integrating random projection with deep learning in industrial UAD. Moreover, unlike other computation-intensive models, RPDP-AD is constructed using a simple MLP network structure. Therefore, it can effectively address the challenge of achieving real-time and high-precision anomaly detection under limited computational resources in the aviation sector. Experiments conducted on a real PRSOV vibration dataset containing seven types of anomalies show that RPDP-AD outperforms other representative UAD algorithms. Sensitivity analysis further validates the stability of the RPDP-AD algorithm under different projection matrices and under noise conditions.

The main contributions can be summarized as follows.

- 1) This article integrates random projection theory with deep neural networks for industrial anomaly detection and health management, which provides new insights to the application of this combined approach.
- 2) This article proposes RPDP-AD: a novel unsupervised PRSOV multifault anomaly detection algorithm based on random projection distance prediction, bridging the gap of lack of UAD methods in a label-free manner for PRSOV.
- 3) This article establishes a theoretical basis for the feasibility of applying inner product prediction with random projection in neural network models based on the Johnson–Lindenstrauss theorem, further enhancing its reliability.
- 4) Experiments over a real world PRSOV dataset including seven different types of anomalies show that RPDP-AD surpasses existing methods across multiple fault types. Sensitivity analysis further validates the stability of RPDP-AD.

The rest of this article is organized as follows. Section II reviews some related work for our study. Section III describes the PRSOV model and the dataset we used. Section IV details the methodology we proposed. We provided theoretical foundation for the inner product preservation property based on the Johnson–Lindenstrauss theorem. Section V outlines our experimental study, which includes an ablation study to determine trade-off parameters, a comparative study with other data-driven approaches and a sensitivity study to discuss RPDP-AD's stability. Section VI concludes this article with an analysis of the main strengths and suggestions for future work.

II. RELATED WORK

A. UAD for Industrial Setting

UAD has been extensively studied, with various methods proposed to identify anomalies in industrial systems without relying on labeled data. For example, Xu et al. [23] proposed an ensemble deep learning approach with model-driven numerical optimization methods for more electric aircraft scheduling. Shang et al. [24] designed a global prior

transformer network for aeroengine blade damage detection. Shao et al. [25] proposes a convolutional deep belief network for electric locomotive bearing fault diagnosis. Zhang et al. [26] proposed an integrated multitasking intelligent tower pumping unit process monitoring scheme for fault detection. Huang et al. [27] developed a bidirectional LSTM prognostics approach for aircraft turbofan engines maintenance. However, the success of these methods highly depends on large amounts of labeled anomalous data. Despite these advancements, current methods often adopt large-scale models, which are unsuitable for deployment in resource-constrained environments like aircraft systems, where real-time analysis is necessary. Moreover, many models lack theoretical support, and there is an absence of UAD methods tailored for PRSOV applications.

B. Random Projection With Deep Learning

Random projection is a fundamental technique in dimensionality reduction. By mapping high-dimensional data to a lower-dimensional space while preserving its geometric properties, it has been widely adopted in various deep learning tasks, including computer vision, graph learning, and time-series analysis. For example, Yang et al. [29] proposed a sparse random projection reconstruction algorithm for compressed imaging with enhanced reconstruction efficiency and less computation costs. Heidari et al. [30] applied random projection to optimize feature selection in machine learning models for breast lesion classification. Hu et al. [31] proposed the random projection heterogeneous graph neural network, which enhances graph learning efficiency while maintaining low information loss. Ma et al. [32] developed random projection recurrent neural networks for time-series classification, tackling the gradient vanishing problem and improving long-term sequence modeling. While random projection has shown great promise in deep learning applications, its industrial adoption for UAD remains largely unexplored. Existing works mainly focus on supervised learning tasks, leaving a gap in applying random projection-based methods to industrial anomaly detection scenarios, especially in unsupervised scenario.

C. Detection Methods for PRSOV

Many studies have explored the application of machine learning tailored for PRSOV anomaly detection. Sano and Berton [33] employed multiple machine learning algorithms such as k-nearest neighbors, artificial neural networks, gradient boosting, Bayesian generalized linear models, and Random Forests to classify PRSOV faults. de Assis Silva et al. [28] investigated the capability of machine learning techniques to perform regression-based anomaly detection for PRSOVs. Their study emphasized the importance of feature selection based on operational and hysteresis parameters, although the selection process remained manual. However, these methods for PRSOV only focus on supervised binary classification, which requires labeled datasets for training. There is a lack for exploration of UAD methods that can better adapt to practical industrial scenarios.

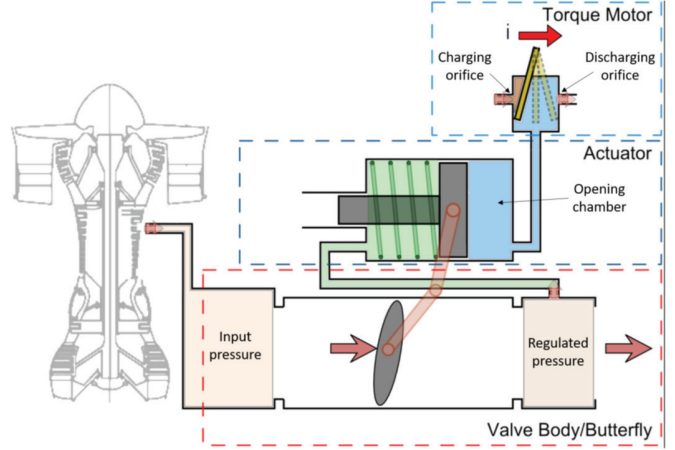


Fig. 1. Schematic of pressure regulating and shutoff valve [28].

III. PRSOV AND DATA DESCRIPTION

A. Pressure-Regulated Shutoff Valves

ECS is a critical system on aircraft which is responsible for regulating and maintaining internal conditions such as temperature, humidity, and airflow. This ensures both passenger comfort and flight safety. The ECS includes functions such as cabin air supply and distribution, pressure control, temperature regulation, and humidity management. The primary air source for the ECS is pressurized bleed air extracted from the compressor section of the aircraft engine. A failure in the ECS can result in incidents such as cabin depressurization or temperature instability. PRSOV is a key component of the ECS, designed to regulate and distribute hot air to various subsystems. Operating under high pressure and high temperature, the internal components of the PRSOV are prone to failure. Fig. 1 illustrates the internal subcomponents of a specific PRSOV model.

Notably, the torque motor current, controlled by the system, enables the pintle to move and regulate airflow to the opening chamber and the discharge orifice (which vents to the external environment). Changes in pressure within the opening chamber drive piston movement, which adjusts the butterfly valve angle and pressure drop. This dynamic mechanism effectively regulates downstream pressure [28]. Failures in the PRSOV can cause issues such as inefficient hot air flow and unstable pressure regulation. For instance, faults in the torque motor's charging or discharging functions can severely impact the PRSOV's ability to maintain proper pressure control.

B. Data Description

Any failure in the ECS directly affects the safety of the aircraft. Since flying with a faulty ECS is strictly prohibited, real-world experiments are not feasible. Therefore, this study uses a rigorously validated PRSOV Simulink model to generate anomalous data under various conditions [33]. Each PRSOV sample is carefully crafted under the guidance of valve experts by manipulating its inherent parameters, such as friction coefficients and the levels of charging and discharging blockages. For each sample, the regulated pressure data at

TABLE I
PRSOV DATASET DESCRIPTIONS WITH DIFFERENT ANOMALY TYPES

Type	Class Name	Numbers
Normal	Training Data	600
	Testing Data	400
Isolated Failures	Charge	1000
	Discharge	1000
Simultaneous Failures	Friction	1000
	Charge and Discharge	1000
	Charge and Friction	1000
	Discharge and Friction	1000
	Charge and Discharge and Friction	1000

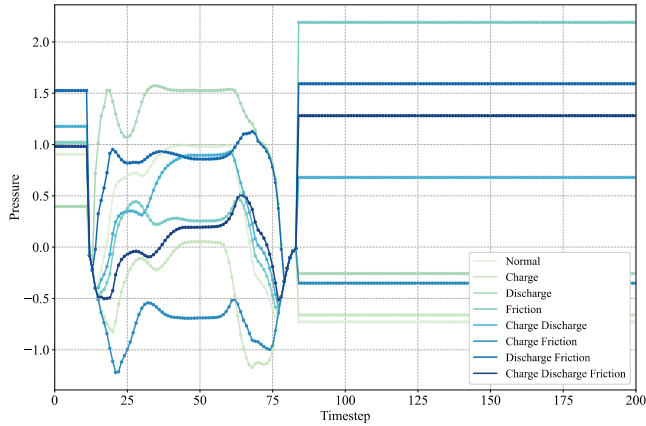


Fig. 2. Examples of PRSOV signals for different class types.

every timestamp are collected as the training input. Each training sample contains 201 pressure-related features. The dataset comprises a total of 8000 training samples, representing eight different health states. Table I summarizes the fault types and their respective sample counts, while Fig. 2 illustrates examples of the collected signal samples. The normal samples were further split into training datasets and testing datasets, while all anomalous types were treated as testing samples.

IV. METHODOLOGY

A. Theoretical Foundation

In this section, we provide a theoretical foundation for our proposed RPDP-AD anomaly detection model. Specifically, we explore the inner product preservation property based on Johnson–Lindenstrauss lemma [34], which links the random projection theory and deep learning neural networks.

Random projection is an efficient dimensionality reduction technique. Given a high-dimensional data matrix $X \in \mathbb{R}^{d \times n}$, where n is the number of data points, and d is the original dimensionality of the data. Random projection utilizes a random matrix A to project the data into a k -dimensional low-dimensional space, where $k \ll d$, achieving dimensionality reduction. The Johnson and Lindenstrauss [34] provide the theoretical foundation for this algorithm. It states that by using a random projection matrix, data points in a high-dimensional space can be projected into a lower-dimensional space while

preserving the distance relationship between data points to a certain extent, which is also strictly proved with mathematics in [17]. The theorem is formulated as follows.

Theorem 1 (Johnson–Lindenstrauss [34]): Let $\epsilon \in (0, 1/2)$. Let $Q \subset \mathbb{R}^d$ be a set of n points and $k = (20 \log n)/\epsilon^2$. There exists a Lipschitz mapping $f: \mathbb{R}^d \rightarrow \mathbb{R}^k$ such that for all $u, v \in Q$

$$(1 - \epsilon)\|u - v\|^2 \leq \|f(u) - f(v)\|^2 \leq (1 + \epsilon)\|u - v\|^2. \quad (1)$$

Subsequently, Theorem 2 explicitly illustrates the Norm preservation property of random projection, which is stated as follows.

Theorem 2 (Norm Preservation [17]): Let $x \in \mathbb{R}^d$. Assume that the entries in $A \in \mathbb{R}^{k \times d}$ are sampled independently of $N(0, 1)$. Then

$$\Pr\left((1 - \epsilon)\|x\|^2 \leq \left\|\frac{Ax}{\sqrt{k}}\right\|^2 \leq (1 + \epsilon)\|x\|^2\right) \geq 1 - 2e^{-\frac{(\epsilon^2 - \epsilon^3)k}{4}}. \quad (2)$$

Theorem 2 requires that the random projection matrix A be sampled independently of a Gaussian distribution. However, Lemma 1 demonstrates that it is not strictly necessary to use a Gaussian distribution. Many other distributions with unit variance and certain boundedness properties (or higher-order moment conditions) are also sufficient.

Lemma 1 [17]: Assume for $A \in \mathbb{R}^{k \times d}$ that each $A_{i,j}$ is uniform on $\{-1, 1\}$ then for any vector

$$\Pr\left(\left\|\frac{1}{\sqrt{k}}Ax\right\|^2 \geq (1 + \epsilon)\|x\|^2\right) \leq \exp\left(-\frac{k}{4}(\epsilon^2 - \epsilon^3)\right) \quad (3)$$

$$\Pr\left(\left\|\frac{1}{\sqrt{k}}Ax\right\|^2 \leq (1 - \epsilon)\|x\|^2\right) \leq \exp\left(-\frac{k}{4}(\epsilon^2 - \epsilon^3)\right). \quad (4)$$

Based on the above theorem and lemma, a straightforward corollary can be derived: inner products are preserved under random projection.

Corollary 1 [17]: Let $u, v \in \mathbb{R}^d$ and that $\|u\| \leq 1$ and $\|v\| \leq 1$. Let $f = (1/\sqrt{k})Ax$, where A is a $k \times d$ matrix, where each entry is sampled i.i.d from a Gaussian $N(0, 1)$ [or from $U(-1, 1)$]. Then

$$\Pr(|u \cdot v - f(u) \cdot f(v)| \geq \epsilon) \leq 4 e^{-\frac{-(\epsilon^2 - \epsilon^3)k}{4}}. \quad (5)$$

The aforementioned theories [17], [34] confirm that random projection can preserve the structure, features, and inner products of the original data. This further provides a solid theoretical foundation for our proposed RPDP-AD anomaly detection method.

B. Random Projection Distance Prediction

From Corollary 1, it can be concluded that the inner product preservation property of random projection spaces retains the latent class structure and feature information of the original data; therefore, RPDP-AD is trained to predict the inner products in the random projection space. It is compelled to represent the latent information within data. Based on this premise, the proposed prediction-based approach provides a

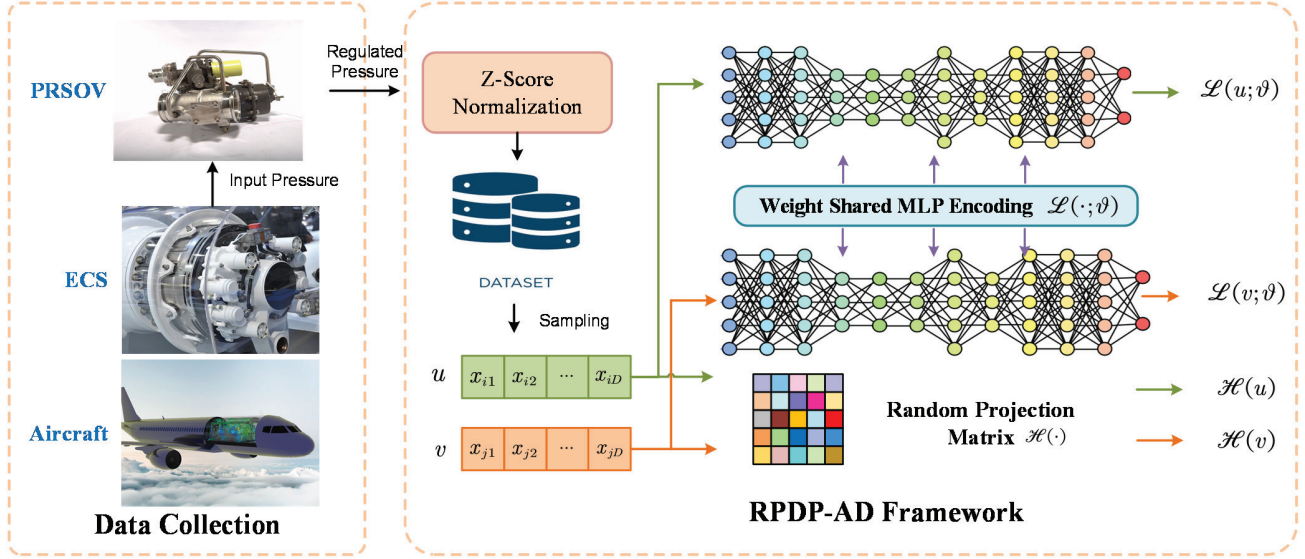


Fig. 3. Workflow of the proposed RPDP-AD framework.

robust supervision signal for training the model without any labels. The proposed RPDP-AD is illustrated in Fig. 3. Assume we obtain a PRSOV dataset $D = \{x_i\}_{i=1}^N$, $x_i \in \mathbb{R}^d$ from real scenarios or aircraft simulation models where N is the total number of samples. We randomly select a pair of samples $u, v \in \mathbb{R}^d$, and input them into a twin network architecture with shared weights. This network is denoted as $\mathcal{L}(\cdot; \vartheta)$ mapping the input samples from the original d -dimensional space into a k -dimensional lower space. Here, ϑ represents the learnable network parameters. Similarly, we establish a random projection function $\mathcal{H}(\cdot)$, which also projects the input samples from the original d -dimensional space into a k -dimensional lower space. To achieve this, RPDP-AD learns the latent structure of the data by minimizing the inner product difference between these two representations in the random projection space. The hidden structural information is represented as follows:

$$L_{IPD}(u, v) = (\mathcal{L}(u; \vartheta) \cdot \mathcal{L}(v; \vartheta) - \mathcal{H}(u) \cdot \mathcal{H}(v))^2. \quad (6)$$

Here, the inner product captures the critical structural relationship between data points, such as their similarity in feature space. This ensures that the encoded model preserves the relationships between samples, even after dimensionality reduction. For anomaly detection tasks, the model utilizes only normal samples and aims to establish the distribution boundaries of these normal samples. RPDP-AD enforces the model to represent distances and similarities in the data space through inner product prediction in the random projection space. This approach allows for the precise encoding of the distribution of normal data patterns. By doing so, the model can effectively learn the inherent structure of normal data, making it easier to detect anomalies that deviate from this learned distribution.

C. Distribution Difference Indicator

As illustrated in Fig. 3, the proposed RPDP-AD uses inner product predictions in the random projection space to capture

the structural and class relationships between samples. To further improve anomaly detection capabilities, an additional distribution difference indicator is introduced. This indicator is defined as follows:

$$L_{DDI}(x) = (\mathcal{L}(x; \vartheta) - \mathcal{H}(x))^2. \quad (7)$$

The objective is to minimize the distributional differences between the neural-network-projected space and the random projection space. This encourages the model to maintain consistency with the latent structure of normal samples. By using normal samples for the above optimization, the model achieves a low distribution difference metric. When new anomalous samples are introduced, the feature structure encoded by the model for normal samples will no longer be applicable, resulting in a significant increase in L_{DDI} . This increase serves as a strong supplementary signal for anomaly detection.

D. Total Loss and Implementation

The multifault anomaly detection model proposed in this study is theoretically grounded in the Johnson–Lindenstrauss lemma. It achieves the distribution encoding of normal patterns through inner product prediction in the random projection space. RPDP-AD employs inner product difference and distribution difference loss functions as supervisory signals to optimize the model's parameters. These are defined as follows:

$$\arg \min_{\vartheta} \sum_{u, v \in D} \lambda_{LPD} L_{IPD}(u, v) + \lambda_{DDI} (L_{DDI}(u) + L_{DDI}(v)) \quad (8)$$

where λ_{LPD} and λ_{DDI} are the weighting parameters of two losses. Given that each PRSOV data sample consists of 201 pressure features, the weight-sharing twin network in RPDP-AD employs a multilayer perceptron to prevent overfitting. More implementation details can be referred to Section V-A.

TABLE II
RPDP-AD PERFORMANCE ON DIFFERENT LOSS WEIGHTS WITH EACH FAULT TYPE DETAILED

Weight Settings $\lambda_{DDI}/\lambda_{IPD}$	Types Metrics	1.Charge	2.Discharge	3.Friction	4.Charge & Discharge	5.Charge & Friction	6.Discharge & Friction	7.Charge & Discharge & Friction	Average
		1.Charge	2.Discharge	3.Friction	4.Charge & Discharge	5.Charge & Friction	6.Discharge & Friction	7.Charge & Discharge & Friction	Average
1:1	AUC	0.994	0.994	0.966	0.958	0.999	0.998	0.996	0.986
	AUPRC	0.998	0.998	0.983	0.977	0.999	0.999	0.998	0.993
	Accuracy	0.988	0.996	0.949	0.945	0.997	0.999	0.986	0.980
	F1-score	0.980	0.972	0.947	0.943	0.996	0.987	0.987	0.973
1.5:1	AUC	0.995	0.995	0.971	0.966	0.999	0.998	0.998	0.989
	AUPRC	0.998	0.998	0.986	0.981	0.999	0.999	0.999	0.994
	Accuracy	0.989	0.997	0.954	0.950	0.998	0.999	0.990	0.985
	F1-score	0.979	0.978	0.951	0.953	0.999	0.988	0.989	0.977
2:1	AUC	0.996	0.995	0.974	0.966	0.999	0.999	0.999	0.990
	AUPRC	0.998	0.998	0.988	0.983	0.999	0.999	0.999	0.995
	Accuracy	0.990	0.998	0.957	0.952	0.999	0.999	0.992	0.986
	F1-score	0.981	0.979	0.955	0.951	0.999	0.990	0.990	0.978
5:1	AUC	0.993	0.996	0.976	0.958	0.999	0.999	0.998	0.988
	AUPRC	0.997	0.998	0.989	0.977	0.999	0.999	0.999	0.994
	Accuracy	0.987	0.997	0.960	0.946	0.999	0.999	0.991	0.983
	F1-score	0.976	0.98	0.955	0.947	0.998	0.994	0.987	0.977
8:1	AUC	0.993	0.997	0.974	0.939	0.999	0.999	0.996	0.985
	AUPRC	0.997	0.999	0.989	0.965	0.999	0.999	0.998	0.992
	Accuracy	0.986	0.998	0.955	0.935	0.999	0.998	0.989	0.980
	F1-score	0.978	0.981	0.951	0.934	0.997	0.994	0.983	0.974
10:1	AUC	0.989	0.995	0.970	0.936	0.999	0.999	0.995	0.983
	AUPRC	0.996	0.998	0.986	0.962	0.999	0.999	0.998	0.991
	Accuracy	0.983	0.997	0.951	0.932	0.999	0.998	0.988	0.978
	F1-score	0.971	0.979	0.947	0.930	0.995	0.991	0.981	0.971
$\lambda_{DDI}=0$	AUC	0.533	0.687	0.576	0.578	0.515	0.641	0.603	0.590
	AUPRC	0.736	0.861	0.771	0.783	0.719	0.830	0.790	0.784
	Accuracy	0.601	0.685	0.654	0.667	0.621	0.723	0.712	0.666
	F1-score	0.726	0.774	0.736	0.741	0.717	0.751	0.756	0.743
$\lambda_{IPD}=0$	AUC	0.989	0.995	0.968	0.916	0.999	0.999	0.994	0.980
	AUPRC	0.995	0.998	0.982	0.954	0.999	0.999	0.997	0.989
	Accuracy	0.982	0.997	0.949	0.920	0.999	0.998	0.987	0.976
	F1-score	0.969	0.978	0.947	0.912	0.996	0.991	0.978	0.967

V. EXPERIMENTAL STUDY

A. Experimental Setup

This section details the experimental studies conducted to validate the effectiveness of our proposed RPDP-AD model. First, we performed an ablation study of the loss components to determine the optimal weight parameters and to investigate the function of each loss component by selectively removing them one by one. Next, we benchmarked the RPDP-AD model against other data-driven approaches. Moreover, a sensitivity study was conducted to explore the stability of our model by applying different random projection matrices. Finally, we tested RPDP-AD's robustness under noise conditions to simulate industrial uncertainty. We employed the following metrics for evaluation: area under the receiver operating characteristic (ROC) curve (AUC), area under the precision-recall curve (AUPRC), accuracy, and F1-Score. The Adam optimizer was used with a learning rate of 0.001, and the batch size was set to 64. All models were implemented using PyTorch framework and Python 3.8, and they were trained for 500 epochs and

tested on a workstation equipped with an RTX 3090 GPU. For data preprocessing, all data samples are preprocessed using Z-Score normalization to ensure uniform scaling across features. For hyperparameters and MLP networks, we followed the MLP setting parameters in [35] with LeakyReLU activation. The random matrix is sampled from standard Gaussian distribution with projected dimension set to 128. However, as discussed before, other distributions with unit variance and certain boundedness properties can also be used. The choice of random projection matrix is discussed in the following sensitivity study.

B. Ablation Study of Loss Components

To validate the effectiveness of the critical loss components in our proposed RPDP-AD approach, this section provides a detailed ablation study on the effect of each loss component, that is, the inner product difference loss function L_{IPD} and the distribution difference loss L_{DDI} on the overall performance of detection. Specifically, we conducted the following experiments by selecting different weighting parameters λ_{LPD} and

λ_{DDI} to investigate how these two loss components influence the anomaly detection ability of the proposed approach. To ensure comprehensiveness, the RPDP-AD was evaluated on the seven types of faults mentioned in Section II. We trained all models in an unsupervised manner, using only normal samples. Afterward, we test each model's performance on different fault types respectively. Table II details the anomaly detection results on each fault type of RPDP-AD with different loss weighting settings.

It could be noted that RPDP-AD demonstrates excellent performance with $\lambda_{DDI} \neq 0$ consistently. However, if we remove the inner product difference loss function by setting $\lambda_{DDI} = 0$, the overall performance of RPDP-AD deteriorated much with average AUC of only 0.590 and only an accuracy of 0.666. This result is reasonable since L_{DDI} attempts to minimize the distribution difference between the MLP network's feature space and the random projection space. If we only consider L_{IPD} constraint with the inner product information, RPDP-AD cannot learn a good statistical representation of normal samples. The introduction of L_{DDI} is essential which ensures that the MLP network's feature mappings could retain the original properties and inner data structure of input samples. On the other hand, the introduction of L_{IPD} is also beneficial for the learning of normal patterns. From Table II, without L_{IPD} , the model achieves an average AUC of 0.980, AUPRC of 0.989, accuracy of 0.976, and $F1$ -score of 0.967. If we add L_{IPD} , the overall performance of RPDP-AD all demonstrate obvious improvement but to varying degrees. This result further proves the efficacy of inner product constraint for latent space learning.

It is also worthwhile to determine the exact weighting parameters λ_{IPD} and λ_{DDI} . Table II shows that when $\lambda_{DDI}/\lambda_{IPD}$ is less than 2:1, the performance of RPDP-AD improves with an increase in the $\lambda_{DDI}/\lambda_{IPD}$ ratio. Conversely, when the ratio of $\lambda_{DDI}/\lambda_{IPD}$ exceeds 2:1, the performance of RPDP-AD declines as the $\lambda_{DDI}/\lambda_{IPD}$ ratio increases. Therefore, we consider 2:1 to be the optimal parameter setting for RPDP-AD. In the following comparative study and sensitivity study, we maintained the 2:1 parameter configuration.

C. Comparative Study With Data-Driven Approaches

In our research, RPDP-AD was also evaluated by comparing it with other representative data-driven anomaly detection approaches. We benchmarked RPDP-AD against other excellent unsupervised machine learning or deep learning-based anomaly detection models, including RCA [36], DeepSVDD [37], GOAD [38], REPEN [39], NeuTraL [40], SLAD [41], IForest [42], ROD [43], ECOD [44], and KDE [45]. Again, we trained all these models in an unsupervised manner with only normal signals, and the testing result was recorded in Table III. The proposed RPDP-AD method demonstrates superior performance compared to other competitors across various metrics, including AUC, AUPRC, accuracy, and $F1$ -score.

Table III shows that RPDP-AD achieves the highest average AUC (0.990), AUPRC (0.953), accuracy (0.986), and $F1$ -score (0.973) among all evaluated approaches. These results indicate that the RPDP-AD consistently outperforms other approaches

in detecting anomalies in PRSOV. The high average AUC score reflects its ability to distinguish between normal and anomalous instances across different types of anomalies. The highest AUPRC score confirms its effectiveness in maintaining high precision and recall, particularly in scenarios with class imbalance. Table III further indicates that RPDP-AD performs fairly well across all seven types of anomalies. It attains near-perfect scores (AUC/AUPRC/Accuracy/ $F1 \geq 0.990$) in type 5 (Charge and Friction) and type 6 (Discharge and Friction), demonstrating robustness to multisource anomaly interactions. It also performs well in type 1 (Charge) with AUC = 0.996 and type 2 (Discharge) with $F1$ -score = 0.979, which can prove its adaptability to both isolated and hybrid fault modes. While baseline methods like SLAD and neutral show competitive performance (average AUC: 0.969 and 0.951), they exhibit 2.7% and 4.8% relative $F1$ -score gaps compared to RPDP-AD, particularly in complex anomalies (e.g., Type 3 Friction: SLAD $F1$ -score = 0.918 versus RPDP-AD = 0.955). Traditional methods like REPEN and RCA suffer significant performance degradation in charge-related anomalies (Type 1 AUC: 0.428 and 0.854), likely due to insufficient feature disentanglement under overlapping failure patterns. IForest and KDE show limited generalizability, with KDE achieving only 0.779 average $F1$ -score.

In conclusion, RPDP-AD consistently achieves superior performance across all types of anomalies in PRSOV. Its highest average scores in AUC, AUPRC, accuracy, and $F1$ -score demonstrate its robustness and reliability. The method's ability to maintain high detection accuracy across various anomaly types, including complex combinations, sets it apart from existing data-driven methods, some of which show significant weaknesses in specific categories.

D. Sensitivity Analysis

1) *Sensitivity Study on the Random Matrices:* In this section, we evaluate the sensitivity of the proposed model to different types of random projection matrices. We investigate the effects of Gaussian random matrices, sparse random matrices, orthogonal random matrices, and discrete random matrices on the model's performance in PRSOV anomaly detection. For each type of random projection matrix.

- 1) *Gaussian Random Matrices:* Elements are sampled independently of a standard Gaussian distribution $\mathcal{N}(0, 1/k)$.
- 2) *Sparse Random Matrices:* Elements are constructed using a sparsity factor s where each entry is assigned values from the following distribution ($s = 3$ in our experiment):

$$A_{ij} = \begin{cases} \sqrt{s}, & \text{with probability } \frac{1}{2s} \\ 0, & \text{with probability } 1 - \frac{1}{s} \\ -\sqrt{s}, & \text{with probability } \frac{1}{2s}. \end{cases} \quad (9)$$

- 3) *Orthogonal Random Matrices:* A dense random matrix $A \in \mathbb{R}^{k \times d}$ is first generated with elements sampled independently of $\mathcal{N}(0, 1)$. The matrix is then orthogonalized using QR decomposition.

TABLE III
EXPERIMENTAL RESULTS ON PRSOV DATASET COMPARED WITH DATA-DRIVEN METHODS

Model	Types Metrics	1.Charge	2.Discharge	3.Friction	4.Charge & Discharge	5.Charge & Friction	6.Discharge & Friction	7.Charge & Discharge & Friction	Average
DeepSVDD	AUC	0.970	0.999	0.978	0.898	0.999	0.998	0.993	0.976
	AUPRC	0.986	0.999	0.989	0.950	0.999	0.999	0.996	0.988
	Accuracy	0.965	0.997	0.971	0.879	0.997	0.997	0.989	0.971
	F1-score	0.942	0.998	0.957	0.893	0.995	0.989	0.977	0.964
REPEN	AUC	0.428	0.927	0.464	0.512	0.415	0.837	0.610	0.599
	AUPRC	0.723	0.959	0.729	0.751	0.724	0.910	0.804	0.800
	Accuracy	0.678	0.908	0.692	0.713	0.669	0.825	0.739	0.746
	F1-score	0.648	0.927	0.668	0.699	0.636	0.848	0.728	0.736
RCA	AUC	0.854	0.918	0.589	0.536	0.933	0.831	0.718	0.768
	AUPRC	0.925	0.960	0.788	0.751	0.964	0.906	0.851	0.878
	Accuracy	0.856	0.902	0.745	0.729	0.920	0.845	0.792	0.827
	F1-score	0.853	0.897	0.735	0.721	0.913	0.852	0.791	0.823
GOAD	AUC	0.884	0.897	0.733	0.920	0.964	0.875	0.837	0.873
	AUPRC	0.942	0.951	0.862	0.778	0.978	0.928	0.910	0.907
	Accuracy	0.889	0.875	0.801	0.784	0.950	0.876	0.843	0.860
	F1-score	0.878	0.886	0.793	0.773	0.944	0.881	0.851	0.858
Neutral	AUC	0.938	0.966	0.911	0.905	0.989	0.975	0.974	0.951
	AUPRC	0.966	0.983	0.949	0.935	0.994	0.987	0.985	0.971
	Accuracy	0.921	0.948	0.908	0.912	0.979	0.967	0.962	0.942
	F1-score	0.822	0.946	0.911	0.915	0.969	0.956	0.957	0.925
SLAD	AUC	0.977	0.992	0.923	0.925	0.998	0.988	0.979	0.969
	AUPRC	0.987	0.997	0.950	0.945	0.998	0.994	0.983	0.979
	Accuracy	0.968	0.990	0.922	0.93	0.996	0.981	0.973	0.966
	F1-score	0.962	0.972	0.918	0.929	0.989	0.975	0.975	0.960
IForest	AUC	0.883	0.923	0.916	0.872	0.930	0.914	0.909	0.907
	AUPRC	0.874	0.936	0.894	0.881	0.946	0.902	0.910	0.906
	Accuracy	0.880	0.915	0.902	0.875	0.928	0.91	0.904	0.902
	F1-score	0.865	0.921	0.901	0.879	0.940	0.906	0.912	0.903
ECOD	AUC	0.954	0.976	0.949	0.926	0.984	0.971	0.957	0.960
	AUPRC	0.926	0.983	0.914	0.921	0.988	0.981	0.966	0.954
	Accuracy	0.938	0.972	0.905	0.916	0.984	0.968	0.955	0.948
	F1-score	0.919	0.971	0.902	0.915	0.988	0.972	0.956	0.946
KDE	AUC	0.813	0.825	0.796	0.688	0.799	0.818	0.783	0.789
	AUPRC	0.821	0.833	0.795	0.763	0.801	0.798	0.762	0.796
	Accuracy	0.787	0.810	0.78	0.715	0.792	0.790	0.771	0.778
	F1-score	0.792	0.820	0.781	0.705	0.795	0.786	0.777	0.779
RPDP-AD	AUC	0.996	0.995	0.974	0.966	0.999	0.999	0.999	0.990
	AUPRC	0.998	0.998	0.988	0.983	0.999	0.999	0.999	0.995
	Accuracy	0.990	0.998	0.957	0.952	0.999	0.999	0.992	0.986
	F1-score	0.981	0.979	0.955	0.951	0.999	0.990	0.990	0.978

4) *Discrete Random Matrices*: Each entry of the matrix A_{ij} is independently sampled from a discrete uniform distribution $A_{ij} \in \{-1, +1\}$ with equal probabilities.

For hyperparameters, the dimension of low-dimensional space is set to 128 (the same as in previous experiments). For robustness, each random projection matrix type is generated using three independent random seeds. Table IV records the average scores (AUC, AUPRC, accuracy, F1-score), for each matrix type across the seven anomaly categories.

The results demonstrate that the proposed model achieves generally good performance across all types of random projection matrices. This indicates RPDP-AD's robustness and stability for PRSOV anomaly detection. Among the matrix

TABLE IV
AVERAGE SCORES ON SEVEN TYPES OF ANOMALIES ACHIEVED BY DIFFERENT RANDOM MATRICES

Method	AUC	AUPRC	Accuracy	F1-score
Gaussian	0.990	0.995	0.986	0.978
Sparse	0.942	0.960	0.938	0.938
Orthogonal	0.974	0.985	0.969	0.965
Discrete	0.885	0.891	0.874	0.861

types, Gaussian random matrices exhibit the best overall performance, with the highest AUC (0.990), AUPRC (0.995), accuracy (0.986), and F1-score (0.978). This is attributed to their strong theoretical guarantees in preserving inner product

TABLE V
AVERAGE SCORES ON SEVEN TYPES OF ANOMALIES UNDER DIFFERENT NOISE LEVELS

Noise (σ^2)	AUC	AUPRC	Accuracy	F1-score
0	0.990	0.995	0.986	0.978
0.05	0.986	0.992	0.982	0.973
0.1	0.977	0.986	0.972	0.968
0.15	0.969	0.975	0.964	0.952

relationships and their ability to accurately project data into a lower-dimensional space while maintaining the inner structure. Orthogonal random matrices follow closely since orthogonality can ensure preservation of geometric properties. However, the added computational cost of orthogonalization may limit their practicality in some scenarios. Sparse random matrices and discrete random matrices perform relatively worse. This is expected since the sparsity and the discretization process inherently result in a significant loss of information. Discrete matrices show the lowest performance because their binary nature limits their ability to capture subtle relationships in the data. In summary, the sensitivity analysis on random matrices demonstrates the stability of RPDP-AD, and it further verifies the effectiveness of the chosen Gaussian random matrix in the above experiments.

2) *Sensitivity Study Under Noise Conditions*: To address potential model uncertainties, such as parameter variations and structural deviations in real industrial scenarios, we further evaluated RPDP-AD's robustness and sensitivity by injecting additive Gaussian noise into raw sensor signals ($\mu = 0, \sigma^2 = 0.05, 0.1, 0.15$). Table V summarizes the average metric value of the seven fault types under different noise levels, where the baseline ($\sigma^2 = 0$) is derived from Table III.

The results in Table V show that the proposed RPDP-AD demonstrates consistent robustness against simulated sensor noise. As shown in the results, its average AUC declines marginally from 0.990 (baseline) to 0.969 ($\sigma^2 = 0.15$), while F1-score decreases by only 2.7% (0.978 \rightarrow 0.942) under the strongest noise. Similarly, AUPRC decreases by only 0.9% (0.995 \rightarrow 0.986), while accuracy and F1-score maintain robust practicality at $\sigma^2 = 0.15$. These results highlight that even under certain levels of noise, all metrics remain above industrial reliability thresholds, validating its adaptability to parameter shifts or measurement errors. The observed resilience can be attributed to RPDP-AD's robust random projection learning ability and the stability of inner production preservation property. This ensures consistent anomaly detection performance in real-world scenarios with imperfect system models or environmental interference.

E. Visualization of Anomaly Score Distribution

To further demonstrate the effectiveness of our proposed method, we provide a visualization of the anomaly scores in this section, as shown in Fig. 4. The histogram illustrates the distribution of anomaly scores output for samples labeled as normal and anomalous in the test set (depicted in different colors). The anomaly scores have been normalized to a range of [0, 1], where a higher score indicates a greater

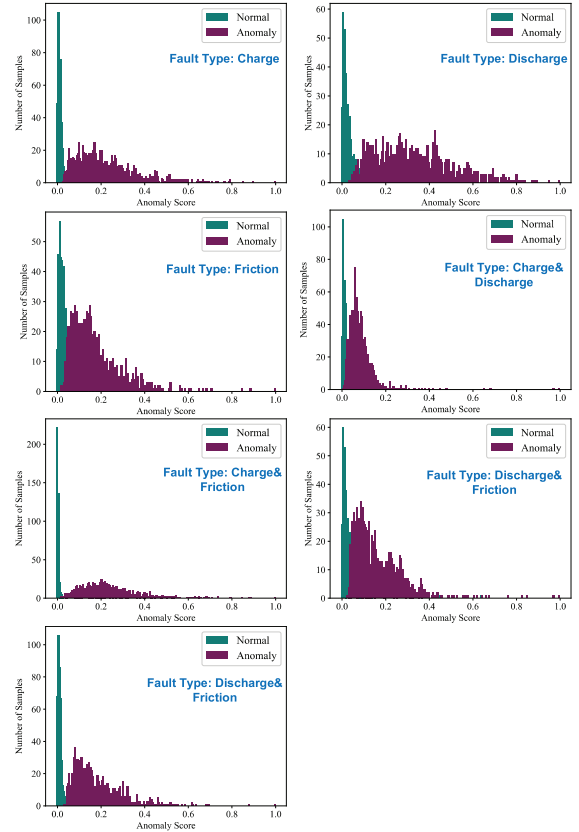


Fig. 4. Visualization of anomaly score distribution on seven fault types.

likelihood that the model considers the sample anomalous. Fig. 4 contains seven subplots, each corresponding to one of the seven types of anomalies tested in our experiments. From the visualization results, it is evident that our model achieves good recognition performance across all anomaly categories. The distribution patterns of normal and anomalous samples are distinct and consistent, showing significant differences. This further confirms that our approach, based on random projection and inner product prediction, provides a robust supervisory signal for anomaly detection. This enables the model to effectively capture the data distribution patterns of normal samples while highlighting the differences presented by anomalous samples. The visualization illustrates that the normal samples tend to cluster around lower anomaly scores, whereas the anomalous samples show higher anomaly scores. This ability to distinguish between different sample types enhances the reliability and accuracy of the anomaly detection process.

F. Limitations of the Experiment

While the experimental results demonstrate the effectiveness of the proposed anomaly detection approach, several limitations should be acknowledged. First, the choice of dataset may influence the outcomes. The experimental data are derived from specific PRSOV operational scenarios, and it is simulated instead of real data, which may not fully capture the variability of real-world conditions. Second, the uniqueness of the experimental scenario may limit the generalizability of the findings. The experiments are conducted under controlled

conditions, which may not include all possible failure modes or external disturbances in practical applications. It is suggested that future work considers testing this method on a broader range of aircraft components and operational conditions to validate its robustness.

VI. CONCLUSION

This article introduces a novel unsupervised aircraft PRSOVs anomaly detection framework based on inner product prediction in random projections. We first provide the theoretical foundation based on Johnson–Lindenstrauss lemma, which links the random projection theory with neural networks. The proposed approach constructs supervisory signals by using distance information (inner product) in a randomly projected space. By inner product prediction in the random projection space, the proposed model encodes class outcomes and sample distance relationships with a simple MLP architecture. We also introduce a distribution difference loss to assist representation learning. Experiments on a real-life PRSOV dataset consisting of seven anomaly types further validated the effectiveness of our model over other data-driven counterparts. The ablation study verified the function of each loss component in the proposed method. The sensitivity study confirmed the stability of our model using different kinds of random projection matrices and various levels of noise injection. Overall, it could be concluded that RPDP-AD can act as a powerful solution for anomaly monitoring of critical aircraft components. Future work could possibly focus on integrating random projection theory with more advanced and novel deep learning backbones for further research as we only consider the simple MLP as a demo in this work.

REFERENCES

- [1] C. M. Ezhilarasu, Z. Skaf, and I. K. Jennions, “A generalised methodology for the diagnosis of aircraft systems,” *IEEE Access*, vol. 9, pp. 11437–11454, 2021, doi: [10.1109/ACCESS.2021.3050877](https://doi.org/10.1109/ACCESS.2021.3050877).
- [2] N. Safaei, “Premature aircraft maintenance: A matter of cost or risk?,” *IEEE Trans. Syst., Man, Cybern., Syst.*, vol. 51, no. 2, pp. 1064–1074, Feb. 2021, doi: [10.1109/TSMC.2019.2895207](https://doi.org/10.1109/TSMC.2019.2895207).
- [3] I. Jennions, F. Ali, M. E. Miguez, and I. C. Escobar, “Simulation of an aircraft environmental control system,” *Appl. Thermal Eng.*, vol. 172, May 2020, Art. no. 114925, doi: [10.1016/j.applthermaleng.2020.114925](https://doi.org/10.1016/j.applthermaleng.2020.114925).
- [4] M. Kordestani, M. E. Orchard, K. Khorasani, and M. Saif, “An overview of the state of the art in aircraft prognostic and health management strategies,” *IEEE Trans. Instrum. Meas.*, vol. 72, pp. 1–15, 2023, doi: [10.1109/TIM.2023.3236342](https://doi.org/10.1109/TIM.2023.3236342).
- [5] E. Zio, “Prognostics and health management methods for reliability prediction and predictive maintenance,” *IEEE Trans. Rel.*, vol. 73, no. 1, p. 41, Mar. 2024, doi: [10.1109/TR.2024.3356816](https://doi.org/10.1109/TR.2024.3356816).
- [6] N. M. Vichare and M. G. Pecht, “Prognostics and health management of electronics,” *IEEE Trans. Compon. Packag. Technol.*, vol. 29, no. 1, pp. 222–229, Mar. 2006, doi: [10.1109/TCAP.2006.870387](https://doi.org/10.1109/TCAP.2006.870387).
- [7] H. Lu et al., “Aircraft detection by a ground-based passive interferometric microwave sensor (PIMS),” *IEEE Trans. Geosci. Remote Sens.*, vol. 61, 2023, Art. no. 5301413, doi: [10.1109/TGRS.2023.3281827](https://doi.org/10.1109/TGRS.2023.3281827).
- [8] P. J. B. Morris and K. V. S. Hari, “Detection and localization of unmanned aircraft systems using millimeter-wave automotive radar sensors,” *IEEE Sensors Lett.*, vol. 5, no. 6, pp. 1–4, Jun. 2021, doi: [10.1109/LSENS.2021.3085087](https://doi.org/10.1109/LSENS.2021.3085087).
- [9] K. Kiraci and E. Akan, “Aircraft selection by applying AHP and TOPSIS in interval type-2 fuzzy sets,” *J. Air Transp. Manage.*, vol. 89, Oct. 2020, Art. no. 101924, doi: [10.1016/j.jairtranman.2020.101924](https://doi.org/10.1016/j.jairtranman.2020.101924).
- [10] S. Zein-Sabatto, J. Bodruzzaman, and M. Mikhail, “Statistical approach to online prognostics of turbine engine components,” in *Proc. IEEE Southeastcon*, Jacksonville, FL, USA, Apr. 2013, pp. 1–6, doi: [10.1109/SSECON.2013.6567479](https://doi.org/10.1109/SSECON.2013.6567479).
- [11] P. Wen, S. Zhao, S. Chen, and Y. Li, “A generalized remaining useful life prediction method for complex systems based on composite health indicator,” *Rel. Eng. Syst. Saf.*, vol. 205, Jan. 2021, Art. no. 107241, doi: [10.1016/j.ress.2020.107241](https://doi.org/10.1016/j.ress.2020.107241).
- [12] E. Naderi and K. Khorasani, “Data-driven fault detection, isolation and estimation of aircraft gas turbine engine actuator and sensors,” *Mech. Syst. Signal Process.*, vol. 100, pp. 415–438, Feb. 2018, doi: [10.1016/j.ymssp.2017.07.021](https://doi.org/10.1016/j.ymssp.2017.07.021).
- [13] J. Hong, Q. Wang, X. Qiu, and H. L. Chan, “Remaining useful life prediction using time-frequency feature and multiple recurrent neural networks,” in *Proc. 24th IEEE Int. Conf. Emerg. Technol. Factory Autom. (ETFA)*, Zaragoza, Spain, Sep. 2019, pp. 916–923, doi: [10.1109/ETFA.2019.8869017](https://doi.org/10.1109/ETFA.2019.8869017).
- [14] S. Shahkar and K. Khorasani, “A multidimensional Bayesian methodology for diagnosis, prognosis, and health monitoring of electrohydraulic servo valves,” *IEEE Trans. Control Syst. Technol.*, vol. 30, no. 3, pp. 931–943, May 2022, doi: [10.1109/TCST.2021.3079198](https://doi.org/10.1109/TCST.2021.3079198).
- [15] P. J. G. Nieto, E. García-Gonzalo, F. S. Lasheras, and F. J. de Cos Juez, “Hybrid PSO–SVM-based method for forecasting of the remaining useful life for aircraft engines and evaluation of its reliability,” *Rel. Eng. Syst. Saf.*, vol. 138, pp. 219–231, Jun. 2015, doi: [10.1016/j.ress.2015.02.001](https://doi.org/10.1016/j.ress.2015.02.001).
- [16] A. Chehade and Z. Shi, “Sensor fusion via statistical hypothesis testing for prognosis and degradation analysis,” *IEEE Trans. Autom. Sci. Eng.*, vol. 16, no. 4, pp. 1774–1787, Oct. 2019, doi: [10.1109/TASE.2019.2897784](https://doi.org/10.1109/TASE.2019.2897784).
- [17] S. Vempala, “Random projection: A new approach to VLSI layout,” in *Proc. 39th Annu. Symp. Found. Comput. Sci.*, May 1998, pp. 389–395, doi: [10.1109/SFCS.1998.743489](https://doi.org/10.1109/SFCS.1998.743489).
- [18] W. Song, W. Shen, L. Gao, and X. Li, “An early fault detection method of rotating machines based on unsupervised sequence segmentation convolutional neural network,” *IEEE Trans. Instrum. Meas.*, vol. 71, pp. 1–12, 2022, doi: [10.1109/TIM.2021.3132989](https://doi.org/10.1109/TIM.2021.3132989).
- [19] B. Li, Y. Wu, J. Song, R. Lu, T. Li, and L. Zhao, “DeepFed: Federated deep learning for intrusion detection in industrial cyber-physical systems,” *IEEE Trans. Ind. Informat.*, vol. 17, no. 8, pp. 5615–5624, Aug. 2021, doi: [10.1109/TII.2020.3023430](https://doi.org/10.1109/TII.2020.3023430).
- [20] H. Ma et al., “Deep-learning-based app sensitive behavior surveillance for Android powered cyber-physical systems,” *IEEE Trans. Ind. Informat.*, vol. 17, no. 8, pp. 5840–5850, Aug. 2021, doi: [10.1109/TII.2020.3038745](https://doi.org/10.1109/TII.2020.3038745).
- [21] N. Zhu, J. Wang, Y. Zhang, H. Wang, and T. Han, “An adversarial training framework based on unsupervised feature reconstruction constraints for crystalline silicon solar cells anomaly detection,” *IEEE Trans. Instrum. Meas.*, vol. 73, pp. 1–13, 2024, doi: [10.1109/TIM.2024.3462989](https://doi.org/10.1109/TIM.2024.3462989).
- [22] J. Zhang, J. Tian, P. Yan, S. Wu, H. Luo, and S. Yin, “Multi-hop graph pooling adversarial network for cross-domain remaining useful life prediction: A distributed federated learning perspective,” *Rel. Eng. Syst. Saf.*, vol. 244, Apr. 2024, Art. no. 109950, doi: [10.1016/j.ress.2024.109950](https://doi.org/10.1016/j.ress.2024.109950).
- [23] B. Xu, F. Guo, L. Xing, Y. Wang, and W.-A. Zhang, “Accelerated and adaptive power scheduling for more electric aircraft via hybrid learning,” *IEEE Trans. Ind. Electron.*, vol. 70, no. 1, pp. 833–845, Jan. 2023, doi: [10.1109/TIE.2022.3150107](https://doi.org/10.1109/TIE.2022.3150107).
- [24] H. Shang, J. Wu, C. Sun, J. Liu, X. Chen, and R. Yan, “Global prior transformer network in intelligent borescope inspection for surface damage detection of aeroengine blade,” *IEEE Trans. Ind. Informat.*, vol. 19, no. 8, pp. 8865–8877, Aug. 2023, doi: [10.1109/TII.2022.3222300](https://doi.org/10.1109/TII.2022.3222300).
- [25] H. Shao, H. Jiang, H. Zhang, and T. Liang, “Electric locomotive bearing fault diagnosis using a novel convolutional deep belief network,” *IEEE Trans. Ind. Electron.*, vol. 65, no. 3, pp. 2727–2736, Mar. 2018, doi: [10.1109/TIE.2017.2745473](https://doi.org/10.1109/TIE.2017.2745473).
- [26] J. Zhang et al., “Process monitoring for tower pumping units under variable operational conditions: From an integrated multitasking perspective,” *Control Eng. Pract.*, vol. 156, Mar. 2025, Art. no. 106229, doi: [10.1016/j.conengprac.2024.106229](https://doi.org/10.1016/j.conengprac.2024.106229).
- [27] C. G. Huang, H. Z. Huang, and Y. F. Li, “A bidirectional LSTM prognostics method under multiple operational conditions,” *IEEE Trans. Ind. Electron.*, vol. 66, no. 11, pp. 8792–8802, Nov. 2019, doi: [10.1109/TIE.2019.2891463](https://doi.org/10.1109/TIE.2019.2891463).
- [28] L. de Assis Silva, H. H. Sano, and C. L. N. Júnior, “Degradation estimation analysis of an aeronautical pneumatic valve using machine learning,” in *Proc. IEEE Int. Syst. Conf. (SysCon)*, Montreal, QC, Canada, Apr. 2022, pp. 1–6, doi: [10.1109/SysCon53536.2022.9773917](https://doi.org/10.1109/SysCon53536.2022.9773917).

- [29] P. Yang, L. Kong, M. Qiu, X. Liu, and G. Chen, "Compressed imaging reconstruction with sparse random projection," *ACM Trans. Multimedia Comput., Commun., Appl.*, vol. 17, no. 1, pp. 1–25, Apr. 2021, doi: [10.1145/3447431](https://doi.org/10.1145/3447431).
- [30] M. Heidari et al., "Applying a random projection algorithm to optimize machine learning model for breast lesion classification," *IEEE Trans. Biomed. Eng.*, vol. 68, no. 9, pp. 2764–2775, Sep. 2021, doi: [10.1109/TBME.2021.3054248](https://doi.org/10.1109/TBME.2021.3054248).
- [31] J. Hu, B. Hooi, and B. He, "Efficient heterogeneous graph learning via random projection," *IEEE Trans. Knowl. Data Eng.*, vol. 36, no. 12, pp. 8093–8107, Dec. 2024, doi: [10.1109/TKDE.2024.3434956](https://doi.org/10.1109/TKDE.2024.3434956).
- [32] Y. Ma, M. Hu, Q. Chang, and H. Lu, "Random projection recurrent neural networks for time series classification," in *Proc. 8th Int. Conf. Electron. Inf. Emergency Commun. (ICEIEC)*, Jun. 2018, pp. 40–43, doi: [10.1109/ICEIEC.2018.8473552](https://doi.org/10.1109/ICEIEC.2018.8473552).
- [33] H. H. Sano and L. Berton, "Application of deep learning models for aircraft maintenance," in *Proc. Anais do XIX Encontro Nacional de Inteligência Artif. Computacional (ENIAC)*, Nov. 2022, pp. 787–797, doi: [10.5753/eniac.2022.227575](https://doi.org/10.5753/eniac.2022.227575).
- [34] W. B. Johnson and J. Lindenstrauss, "Extensions of Lipschitz mappings into Hilbert space," *Contemp. Math.*, vol. 26, pp. 189–206, Jan. 1984.
- [35] H. Wang, G. Pang, C. Shen, and C. Ma, "Unsupervised representation learning by predicting random distances," 2019, *arXiv:1912.12186*.
- [36] B. Liu, D. Wang, K. Lin, P.-N. Tan, and J. Zhou, "RCA: A deep collaborative autoencoder approach for anomaly detection," in *Proc. 30th Int. Joint Conf. Artif. Intell.*, Aug. 2021, pp. 1505–1511, doi: [10.24963/ijcai.2021/208](https://doi.org/10.24963/ijcai.2021/208).
- [37] L. Ruff et al., "Deep one-class classification," in *Proc. 35th Int. Conf. Mach. Learn.*, 2018, pp. 4393–4402. Accessed: Jun. 5, 2024. [Online]. Available: <https://proceedings.mlr.press/v80/ruff18a.html>
- [38] L. Bergman and Y. Hoshen, "Classification-based anomaly detection for general data," in *Proc. Int. Conf. Learn. Represent. (ICLR)*, 2020, pp. 1–12.
- [39] G. Pang, L. Cao, L. Chen, and H. Liu, "Learning representations of ultrahigh-dimensional data for random distance-based outlier detection," in *Proc. 24th ACM SIGKDD Int. Conf. Knowl. Discovery Data Mining*, Jul. 2018, pp. 2041–2050, doi: [10.1145/3219819.3220042](https://doi.org/10.1145/3219819.3220042).
- [40] Q. Chen, T. Pfommer, M. Kloft, S. Mandt, and M. Rudolph, "Neural transformation learning for deep anomaly detection beyond images," in *Proc. Int. Conf. Mach. Learn.*, Jan. 2021, pp. 8703–8714.
- [41] H. Xu, Y. Wang, J. Wei, S. Jian, Y. Li, and N. Liu, "Fascinating supervisory signals and where to find them: Deep anomaly detection with scale learning," in *Proc. 40th Int. Conf. Mach. Learn.*, Honolulu, HI, USA, 2023, pp. 38655–38673.
- [42] F. T. Liu, K. M. Ting, and Z.-H. Zhou, "Isolation forest," in *Proc. 8th IEEE Int. Conf. Data Mining*, Apr. 2008, pp. 413–422, doi: [10.1109/ICDM.2008.17](https://doi.org/10.1109/ICDM.2008.17).
- [43] Y. Almardeny, N. Boujnah, and F. Cleary, "A novel outlier detection method for multivariate data," *IEEE Trans. Knowl. Data Eng.*, vol. 34, no. 9, pp. 4052–4062, Sep. 2022, doi: [10.1109/TKDE.2020.3036524](https://doi.org/10.1109/TKDE.2020.3036524).
- [44] Z. Li, Y. Zhao, X. Hu, N. Botta, C. Ionescu, and G. Chen, "ECOD: Unsupervised outlier detection using empirical cumulative distribution functions," *IEEE Trans. Knowl. Data Eng.*, vol. 35, no. 12, pp. 12181–12193, Dec. 2023, doi: [10.1109/TKDE.2022.3159580](https://doi.org/10.1109/TKDE.2022.3159580).
- [45] L. J. Latecki, A. Lazarevic, and D. Pokrajac, "Outlier detection with kernel density functions," in *Machine Learning and Data Mining in Pattern Recognition*, P. Perner, Ed., Heidelberg, Germany: Springer, 2007, pp. 61–75.



Dandan Peng received the B.Sc. and M.Sc. degrees in mechanical engineering from the University of Electronic Science and Technology of China, Chengdu, China, in 2016 and 2019, respectively, and the Ph.D. degree in mechanical engineering from KU Leuven, Leuven, Belgium, in 2025.

She is currently a Post-Doctoral Researcher, working on battery fault diagnosis by integrating physical models with deep learning. She has published over 30 peer-reviewed articles, including several ESI Highly Cited Papers. Her research interests include prognostics and health management (PHM), anomaly detection, domain adaptation, and interpretable machine learning.

Dr. Peng received awards such as the EAWE Scholarship and ASME Turbo Expo Student Travel Award. She serves on the Youth Editorial Board of several journals and reviews for over 40 international journals.



Ning Zhu was born in Jiangsu, China, in 2003. He is currently pursuing the B.S. degree in electronic and information engineering with the University of Electronic Science and Technology of China, Chengdu, China.

His research interests include machine learning, medical image processing, and anomaly detection.



Te Han (Member, IEEE) received the B.Sc. and Ph.D. degrees in energy and power engineering from Tsinghua University, Beijing, China, in 2015 and 2020, respectively.

He currently holds the position of Associate Professor with the School of Management and Economics, Beijing Institute of Technology, Beijing. Prior to this, he served as a Post-Doctoral Research Fellow at the Department of Industrial Engineering, Tsinghua University, from 2020 to 2023. In 2019, he was a Visiting Scholar at the University of Alberta, Edmonton, AB, Canada. He has authored and co-authored two books and more than 50 articles in technical journals and conference proceedings. His research interests include big data-driven prognostics and health management, reliability analysis, as well as scientific machine learning.

Dr. Han has been recognized as one of the World's Top 2% Scientists by Stanford University consecutively from 2020 to 2022. In addition, he has previously served as a guest editor for internationally renowned SCI journals such as "*Reliability Engineering and System Safety*" and "*Journal of Risk and Reliability*".



Zhuyun Chen (Member, IEEE) received the Ph.D. degree in mechanical engineering from the South China University of Technology, Guangzhou, China, in 2020.

From 2017 to 2018, he was an International Scholar at KU Leuven, Leuven, Belgium, supported by the Elite Youth Program of the Guangzhou Government. From 2020 to 2024, he worked as a Research Associate and a Post-Doctoral Researcher at the School of Mechanical and Automotive Engineering, South China University of Technology. He is currently an Associate Professor with the School of Electromechanical Engineering, Guangdong University of Technology, Guangzhou, China. He has published over 50 papers (including nine ESI highly cited papers), issued more than ten Chinese invention patents. His research interests include dynamic signal processing, intelligent fault diagnosis and health management, digital twin (DT)-assisted industrial data processing, and diagnosis techniques.

Dr. Chen holds the Associate Editor of *IEEE TRANSACTIONS ON INSTRUMENTATION AND MEASUREMENT*, Young editorial boards of various journals, including the Chinese Journal of Mechanical Engineering and the Journal of Dynamics, Monitoring and Diagnostics and Instrumentation. Additionally, he serves as over nine Guest Editors, such as Measurement Science and Technology and Nondestructive Testing and Evaluation, and IET Science, Measurement and Technology. He is the principal investigator (PI) of ten projects which are funded by National Natural Science Foundation of China, Young Talent Support Project of Guangzhou Association for Science and Technology, and University-Industry Cooperation.



Chenyu Liu received the B.S. and M.Sc. degrees from Northwestern Polytechnical University (NPU), Xi'an, China, in 2013 and 2017, respectively, and the Ph.D. degree in mechanical engineering from KU Leuven, Leuven, Belgium, in 2023.

He is currently a Professor with the School of Mechanical and Electrical Engineering, NPU. His research interests include artificial intelligence for intelligent operation and maintenance, including intelligent fault diagnosis, nondestructive testing of aerospace materials, and health monitoring of aerospace equipment. He has extensive experience in data-driven condition monitoring, rotating machinery prognostics, and machine learning applications in engineering systems.